

# Wave packet dynamics in molecular excited electronic states

**Alicia Palacios**

Departamento de Química, Universidad Autónoma de Madrid, 28049 Madrid, Spain

E-mail: [alicia.palacios@uam.es](mailto:alicia.palacios@uam.es)

**Alberto González-Castrillo**

Departamento de Química, Universidad Autónoma de Madrid, 28049 Madrid, Spain

**Henri Bachau**

Centre des Lasers Intenses et Applications, CNRS-CEA-Université de Bordeaux 1, F-33405, Talence, France

**Fernando Martín**

Departamento de Química, Universidad Autónoma de Madrid, 28049 Madrid, Spain  
Instituto Madrileño de Estudios Avanzados en Nanociencia, Cantoblanco, 28049 Madrid, Spain

**Abstract.** We theoretically explore the use of UV pump - UV probe schemes to resolve in time the dynamics of nuclear wave packets in excited electronic states of the hydrogen molecule. The pump pulse ignites the dynamics in singly excited states, that will be probed after a given time delay by a second identical pulse that will ionize the molecule. The field-free molecular dynamics is first explored by analyzing the autocorrelation function for the pumped wave packet and the excitation probabilities. We investigate both energy and angle differential ionization probabilities and demonstrate that the asymmetry induced in the electron angular distributions gives a direct map of the time evolution of the pumped wave packet.

## 1. Introduction

The new generation of laser sources using high-harmonic generation (HHG) techniques [1, 2, 3] and free electron lasers (FEL and X-FEL) [4, 5, 6] nowadays provide intense ultrashort pulses with wavelengths within the UV and XUV energy regions such that one or few-photon absorption promotes electrons into excited states or into the ionization continua of atoms and molecules. The availability of these pulses with durations of the order of a few femtoseconds ( $1 \text{ fs} = 10^{-15} \text{ s}$ ) and even tens of attoseconds ( $1 \text{ as} = 10^{-18} \text{ s}$ ) makes possible to explore the molecular dynamics associated to excited/ionized targets at the time scales at which electrons and fast nuclei move [7, 8, 9]. In the lightest molecules,  $\text{H}_2$  and  $\text{D}_2$ , nuclei move on time-scales of a few tens of femtoseconds (e.g., the vibrational period associated to the ground state of  $\text{H}_2^+$  is around 20 fs). These time scales make hydrogenic molecules particularly interesting targets to explore combined electron and nuclear wave packets using these laser sources [10, 9]. Several recent



experiments used IR pulses to probe and steer the wave packet motion of the electron ejected upon ionizing a  $H_2$  (or  $D_2$ ) molecule with a single attosecond pulse [11] or a train of attosecond pulses [12, 13]. Similar experiments have used pump-probe schemes with two XUV few-fs pulses, where the pump ionizes a hydrogenic molecule and the probe captures a time-resolved image of the nuclear wave packet (NWP) pumped in the molecular ion by analyzing the signal after the Coulomb explosion of the system [14, 15]. In the present work, we propose a similar scheme, but instead of probing the single ionization channels we will use them as the signal to probe singly excited states of the neutral molecule. We thus propose a pump-probe set-up, outlined in Fig. 1, such that the pump pulse excites the molecular target creating a nuclear wave packet in the lowest excited electronic states of the neutral. After promoting one electron into an excited state, the nuclei will vibrate reaching larger internuclear distances. The field-free wave packet then evolves until a second pulse is absorbed leading to ionization. The challenge is to disentangle the contribution from several ionization channels to uncover the signature of the NWP that we seek to probe [16].

Specficially, we will perform a set of simulations with different time delays between two identical pulses with a duration of 2 fs, intensity of  $10^{12}$  W/cm<sup>2</sup> and a central energy of 12.2 eV. This is the energy and bandwidth that is required to create a NWP containing a manifold of vibrational states in the excited target. The pulse duration and intensity, as well as the fact of using identical pulses, are chosen to simulate a realistic experiment considering the current state-of-the-art laser sources [5, 6, 17]. The present manuscript is organized as follows. In

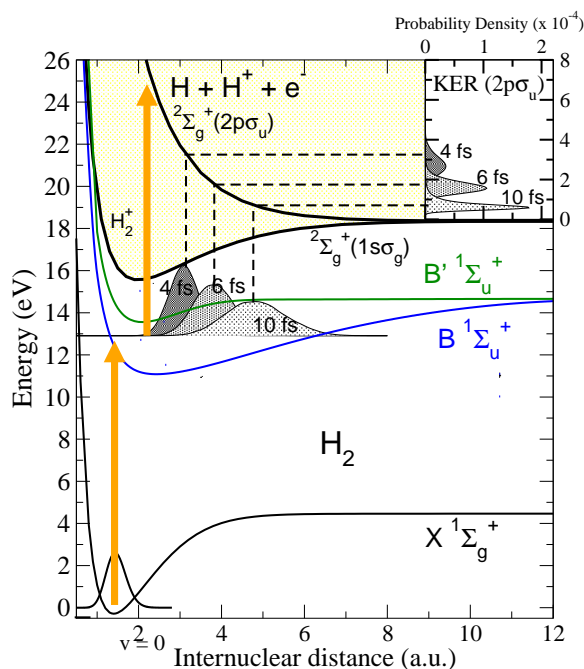


**Figure 1.** Pump-probe scheme (each pulse represented with an arrow) including the relevant potential energy curves of the hydrogen molecule. The pump pulse creates a wave packet containing several vibrational states in the first two excited electronic states of the molecule ( $B$  and  $B'1\Sigma_u^+$ ). The pumped NWP obtained in the calculation is plotted 4, 6 and 10 fs after the pump pulse is absorbed. The probe pulse ionizes the molecule through the first and second (depending on the time delay) ionization thresholds. Dashed lines indicate the one-photon absorption from the probe pulse mapping the NWP into the second ionization threshold ( $2p\sigma_u$ ). For comparison we plot in the inset the calculated probability distributions for this channel ( $2p\sigma_u$ ) for each of the given time delays in the figure.

the next section, an overview of the theoretical method, computational details and current implementation are given. In section 3, we show the excitation probabilities and investigate the dynamics of the pumped wave packet associated to excited electronic states. Section 4 is devoted to analyze the single ionization observables, differential in both energy and angle of the ejected particles, showing the UV-induced asymmetry that traces the pumped dynamics [16]. Finally, we will summarize the main conclusions extracted from this work.

## 2. Methodology

A time-dependent treatment is required to describe the molecular dynamics induced and probed with ultrashort pulses. Our theoretical method has been successfully employed in the context of one- and multi-photon single ionization of hydrogenic molecules by combining pulsed radiation sources in the range of frequencies from the IR to XUV regions [11, 13, 18]. The time-dependent numerical approach is developed in [18, 19], whereas the Feshbach-like formalism employed for the description of the molecular structure is explained in detail in [20, 21]. In the following, we restrict ourselves to the most relevant stages of the method. Note that atomic units are used through the text under otherwise stated.

We solve the time-dependent Schrödinger equation (TDSE), which in its general form is written as:

$$i \frac{\partial}{\partial t} \Phi = \hat{H} \Phi \quad (1)$$

where  $\Phi$  is the wave function of the quantum system and  $\hat{H}$  is the Hamiltonian operator. We seek to explore the dynamics of a wave packet of molecular singly excited states that is both launched and probed by interaction with ultrashort pulses. Therefore, we can solve the TDSE using a non-relativistic Hamiltonian describing both electronic and nuclear degrees of freedom on a molecule using a quantum time-dependent treatment. The pulsed radiation however is supposed intense enough, with a high density of photons, such that the electromagnetic field is treated classically. The TDSE is then written as:

$$i \frac{\partial}{\partial t} \Phi(\mathbf{r}, R, t) = [\hat{H}_0(\mathbf{r}, R) + \hat{V}(\mathbf{r}, t)] \Phi(\mathbf{r}, R, t) \quad (2)$$

where  $\hat{H}_0(\mathbf{r}, R)$  is the field-free Hamiltonian of  $H_2$  and  $\hat{V}(\mathbf{r}, t)$  is the radiation-molecule interaction term. This term is treated within the dipole approximation, which is valid for the wavelengths in the UV and XUV regions here used. We can thus write it in the velocity gauge as:

$$\hat{V}(\mathbf{r}, t) = \hat{\mathbf{A}}(t) \cdot \hat{\mathbf{p}} \quad (3)$$

where  $\hat{\mathbf{p}}$  is the momentum operator for the electron and  $\hat{\mathbf{A}}(t)$  is the vector potential of the field that can be written as:

$$\hat{\mathbf{A}}(t) = \begin{cases} A_0 F(t) \sin(\omega t) \hat{\epsilon} & t \in [0, T] \\ 0 & \text{elsewhere,} \end{cases} \quad (4)$$

where  $\hat{\epsilon}$  is the polarization vector,  $T$  is the duration of a given pulse, and  $F(t)$  is the temporal envelope for the finite pulse for which we use a sine squared function,  $F(t) = \sin^2(\pi t/T)$ . We will use two identical pulses as defined in Eq.4 with a given time delay  $\tau$  among them.

The field-free hamiltonian  $\hat{H}_0$  is separated in the nuclear and electronic terms,  $\hat{H}_0(\mathbf{r}, R) = \hat{T}(R) + \hat{H}_{el}(\mathbf{r}, R)$ , where  $\hat{T}(R) = -\hat{\nabla}_R^2/2\mu$  is the nuclear kinetic energy,  $\mu$  the reduced mass of the nuclei, and  $\hat{H}_{el}$  is the electronic Hamiltonian including the nucleus-nucleus repulsion potential term. Note that we will only neglect the non-adiabatic couplings in our description. The time-dependent wave function in Eq. (2) is expanded in a basis of fully correlated vibronic states obtained from diagonalizing the hamiltonian of the isolated molecule:

$$\Phi(\mathbf{r}, R, t) = \sum_n \sum_{v_n} C_{nv_n}(t) \Psi_{nv_n}(\mathbf{r}, R) e^{-iW_{nv_n}t} + \sum_{\alpha} \sum_{\ell_{\alpha}} \int d\varepsilon_{\alpha} \sum_{v_{\alpha}} C_{\alpha\varepsilon_{\alpha}v_{\alpha}}^{\ell_{\alpha}}(t) \Psi_{\alpha\varepsilon_{\alpha}v_{\alpha}}^{\ell_{\alpha}}(\mathbf{r}, R) e^{-iW_{\varepsilon_{\alpha}v_{\alpha}}t} \quad (5)$$

where  $\Psi_{nv_n}(\mathbf{r}, R)$  corresponds to the  $n$ -th bound (singly or doubly excited) electronic state of  $H_2$  at its  $v_n$  (bound or dissociative) vibrational state and  $\Psi_{\alpha\varepsilon_{\alpha}v_{\alpha}}^{\ell_{\alpha}}(\mathbf{r}, R)$  is an electronic continuum state

of energy  $\varepsilon_\alpha$  in the  $\alpha$  ionization channel at its  $v_\alpha$  (bound or dissociative) vibrational state for an angular momentum  $\ell_\alpha$  of the ejected electron.  $W_x$  stands for the total energy of a given vibronic state. These basis of eigenstates is obtained within the Born-Oppenheimer approximation, with  $\Psi(\mathbf{r}, R) = \phi(\mathbf{r}, R)\chi(R)$ , where  $\phi(\mathbf{r}, R)$  is the electronic and  $\chi(R)$  the vibrational eigenfunction. By substituting the expansion in Eq. (5) into Eq. (2), the problem is reduced to a system of coupled differential equations that can be solved using ordinary integration procedures. A sixth-order Runge-Kutta algorithm, implemented in PETSc libraries [22], is used for the time integration.

As previously mentioned, the electronic structure is obtained within the Feshbach formalism [23]. In brief, two orthogonal complementary subspaces are defined ( $\hat{Q} + \hat{P} = 1$ ), respectively containing the resonant/bound ( $\hat{Q}$ ) and non-resonant ( $\hat{P}$ ) contribution to the continuum electronic wave function at a given energy, and the electronic eigenvalue problem is separately solved for each subspace (see [20, 21, 19] for details). The eigenvalue problem for the  $\hat{Q}$  subspace is solved using a configuration interaction method in a basis of  $H_2^+$  orbitals, whereas for the  $\hat{P}$  subspace we need a more complicated multichannel  $L^2$  close-coupling procedure [24, 21] to properly describe the non-resonant continuum electronic states in the same basis. The basis set of  $H_2^+$  orbitals are written as single center expansions using spherical harmonics for the angular part and B-spline basis functions for the radial part [25, 26]. We found that the present results are converged when using angular momenta expansions up to  $\ell = 16$ , and up to 180 B-splines functions of order  $k = 8$  in a box of size 60 a.u. For the close-coupling procedure, angular momenta of the ejected electron are included up to  $l_\alpha = 7$ , for each  $\alpha$  electronic state in the discretized continua associated to each ionization threshold of the  $H_2^+$  molecule. The nuclear motion is included by solving the one-dimensional Schrödinger equation. We have computed the nuclear wave functions ( $\chi_{v_i}(R)$  where  $v$  is the vibrational state associated to the  $i$ -th electronic state) in a basis set of 300 B-splines defined in a box of size 12 a.u., which is large enough for our present simulations.

Because the computed wave packet in Eq. (2) is written in terms of the stationary states of the system, the expansion coefficients directly give the corresponding (excitation/ionization) amplitudes, which allows for a straightforward analysis of the spectral components (total, energy- and angle-differential) in a given wave packet. Therefore, for a given final energy  $W_{\varepsilon_\alpha v_\alpha}$ , and a given energy sharing for nuclei ( $E_{v_\alpha}$ ) and electrons ( $\varepsilon_\alpha$ ) such as  $W_{\varepsilon_\alpha v_\alpha} = E_{v_\alpha} + \varepsilon_\alpha$ , the ionization probability is:

$$\frac{d^2 P^{\ell_\alpha}(E_{v_\alpha}, \varepsilon_\alpha, T)}{dE_{v_\alpha} d\varepsilon_\alpha} = |C_{\alpha \varepsilon_\alpha v_\alpha}^{\ell_\alpha}(t = t_{max})|^2, \quad (6)$$

where  $\ell_\alpha$  stands for the  $\ell$  angular momentum contribution of the ejected electron in the  $\alpha$  ionization threshold, and  $T$  is the pulse length. To ensure that the wave function has reached its asymptotic limit, we propagate up to a time,  $t_{max} > T$ , larger than the pulse duration.

### 3. Pumped wave packet dynamics

We aim to investigate the dynamics associated to excited states of  $H_2$  in a UV-pump/UV-probe scheme by analyzing the ionization probabilities. It is then worth to first examine the excitation probabilities, as well as the time evolution that follows the pumped NWP, before the interaction of the probe. The absorption of a single photon of 12.2 eV is in resonance with the vertical transition from the ground state to the  $B^1\Sigma_u^+$  state at the equilibrium internuclear distance of  $H_2$  (1.4 a.u.). We simulate the interaction with linearly polarized light parallel to the molecular axis. According to the dipole selection rules, the only molecular states optically allowed in a transition by absorption of an even (odd) number of photons are those of total symmetry  $\Sigma_g^+$  ( $\Sigma_u^+$ ). The relevant potential energy curves are all plotted in Fig. 1.

Because the pulse has an energy bandwidth (2 fs of duration implies an energy bandwidth

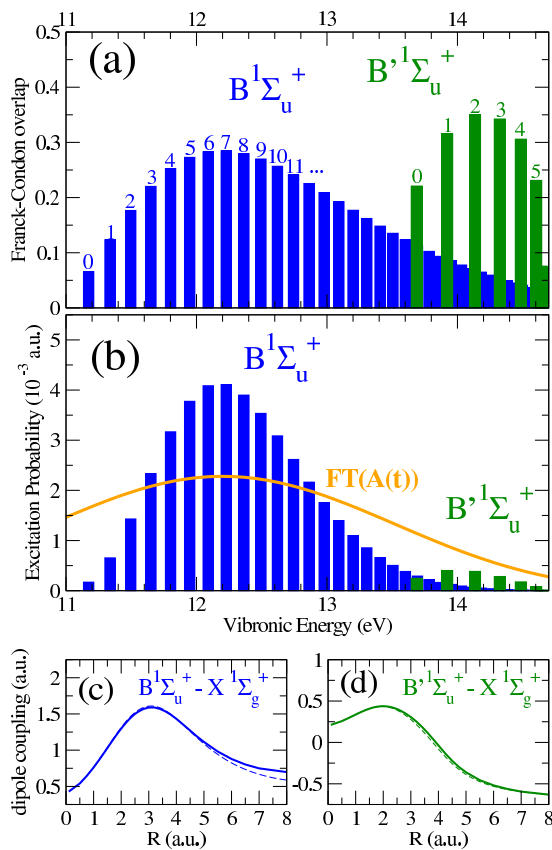


**Figure 2.** (a) Franck-Condon overlaps between the bound vibrational states associated to the electronic excited states B and B' and the ground state of the hydrogen molecule. (b) Excitation probability as a function of the vibrational bound states for the B and B' states. The full orange line in (b) corresponds to the Fourier Transform of the pump pulse (2 fs of duration, intensity of  $10^{12}$  W/cm<sup>2</sup> and 12.2 eV of central frequency), which together with the Franck-Condon overlaps plotted in (a) explains the probability distribution. (c) and (d) are the electronic dipole couplings as a function of internuclear distances from the ground state of the neutral ( $X^1\Sigma_g^+$ ) to each of the B and B' excited states with  $^1\Sigma_u^+$  symmetry. Full lines are present results. Dashed lines: results from reference [27] for comparison.

at around 3 eV) a bunch of vibrational states might be populated not only in the B state, but also in the second electronic excited state, the  $B'^1\Sigma_u^+$  state. The deeper and wider well of the B state holds a larger progression of vibrational states. The population of these states will obviously depend on both electronic and nuclear coordinates. This is illustrated in Fig. 2 where we separately plot the vibrational overlaps (Fig. 2a) and the electronic couplings (Fig. 2c and 2d). Fig. 2a shows the vibrational distribution expected by only considering the Franck-Condon overlaps, i.e., the integral over all the internuclear distances of the product of the vibrational ground state ( $v = 0$  in  $X^1\Sigma_g^+$ , plotted in Fig. 1) to each vibrational bound state associated to the B and B' electronic states. These are compared with the computed excitation probability distributions plotted in Fig. 2b for one single pulse with the parameters given above. We can see that the relative populations between vibrational states associated to a given electronic state B or B', are mainly governed by the Franck-Condon overlaps together with the energy bandwidth of the pulse. The Fourier transform of the field, as defined in Eq. (4) for a 2 fs pulse and centered at 12.2 eV, is also plotted as a full orange line. However, an appropriate description can only be achieved by including the electronic dipole couplings and its dependence with  $R$ . These are plotted in Fig. 2(c) and (d). The oscillator strength to the B state is approximately three times larger than the B', thus explaining the very low excitation probabilities in the B' vibrational states. For both B and B' states, the electronic coupling appreciably decrease for  $R > 3$ , which together with the FC overlaps explains the fast and sharp decrease of population as the vibrational quantum number becomes higher.

In the absence of field, the population of the pumped states shown in Fig. 2(b) remains, and the only time dependency is that one associated to the stationary phases. The values of relative phases between the states contained in the NWP will lead to an initial spread of the NWP (the larger the anharmonicity of the potential energy curve the wider the spreading) and

succeeding partial reconstructions (revivals) in time. The degree of reconstruction will depend on the number of states involved and shape of the potential curve. The revival times, when the NWP is localized in the inner turning point, are mainly given by the average period of the most populated vibrational states. For a quantitative image of the NWP evolution, we define the autocorrelation function for the pumped NWP as:

$$R(\Delta t) = \langle \Psi_m(t = T) | \Psi_m(t = T + \Delta t) \rangle \quad (7)$$

where at a given time ( $t = T + \Delta t$ ) the field-free evolving NWP is projected into the NWP right at the end of the pulse [ $\Psi_m(T) = \sum_{v_m} c_{m,v_m}(T) \chi_{v_m}(R)$ ].  $\Delta t$  is the elapsed time after the end of the pump pulse and  $\tau$  is the time delay between center of the pulses, i.e.,  $t = T + \Delta t = T/2 + \tau$ .

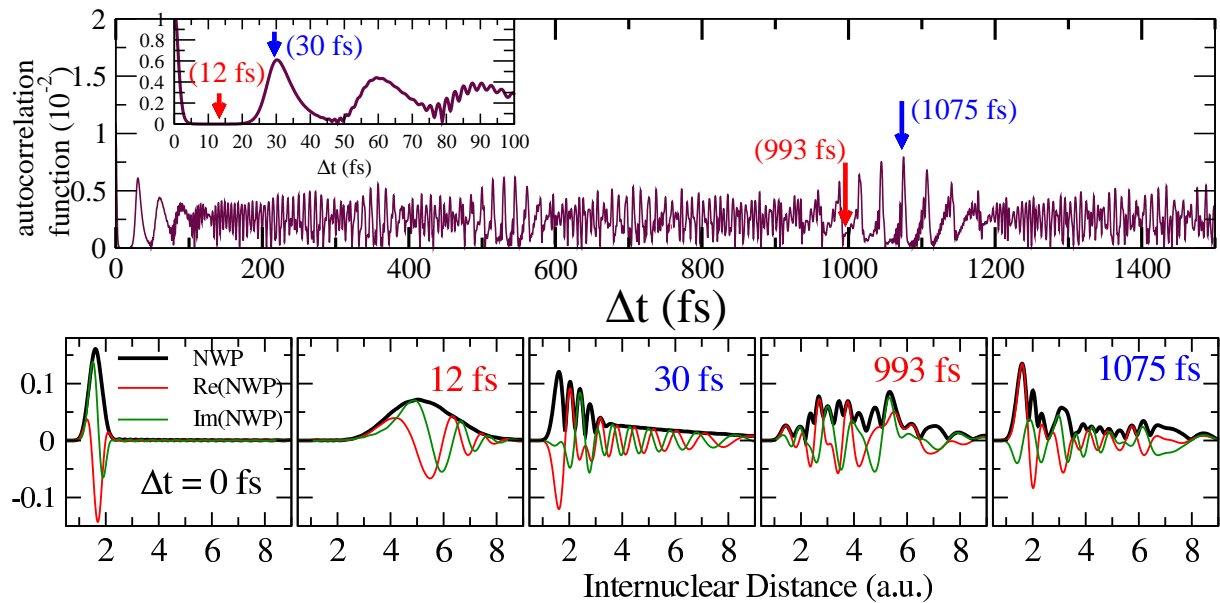


**Figure 3.** (Above) Autocorrelation function as defined in Eq. (7) for the NWP associated to the  $B^1\Sigma_u^+$  electronic state as a function of time delay. (Below) NWP at different times after the absorption of the pump pulse. The real and imaginary components of the NWP are plotted in colors, and absolute value in black thick line.

In Fig. 3 we plot the autocorrelation function as a function of  $\Delta t$  up to 1.5 picoseconds. After 5 fs, the nuclei have already moved apart reaching distances to 4 a.u. We find partial revivals of the wave packet every 30 fs (averaged period in the  $v = 5 - 7$  vibrational states of the B state) with the largest revival being at around 1075 fs ( $R(1075) \approx 0.075$ ). The NWP computed right at the end of the pulse, as well as the two maxima (largest revivals) and two of the minima found in the autocorrelation function are plotted in the lower panel in Fig. 3. To observe the phases we plot in colors both the real and the imaginary part of the NWP,  $\Psi_m(t = T + \Delta t)$ , and its absolute value (black thick line). For the minima at  $\Delta t = 12$  fs the amplitude is zero in the internuclear distances where the initial NWP is located. Other minima, such the one plotted at  $\Delta t = 993$  fs, have non-zero amplitudes but phases that destructively interfere with respect to the initial NWP. For the two maxima, at 12 and 1075 fs, the maximum absolute value of the NWP matches that at  $\Delta t = 0$  fs, but more importantly the phases add up coherently. At this point, the challenge is to find experimentally measurable observables that can access this information. Those are the energy and angle differential single ionization signals, as previously



pointed out in [16]. Due to the photon energies that are required to pump and excite  $\text{H}_2$ , the absorption of both pump and probe leads to single ionization, leaving the ion behind its ground or excited states, or even launching autoionization processes. In the following, we give an extended analysis on the information encoded in the differential ionization probabilities.

#### 4. Energy and angular differential ionization probabilities

The single ionization probabilities as a function of proton kinetic energy (PKE) are plotted in the left panels of Fig. 4 for different time delays. We include the contributions to the first two ionization thresholds ( $1s\sigma_g$  and  $2p\sigma_u$ ). The second ionization threshold is only reached after 4 fs of delay, when the nuclei have moved to internuclear distances such that the energy gap from the excited state to the  $2p\sigma_u$  potential energy curve low enough to be accessible by the probe pulse (see Fig. 1). The  $2p\sigma_u$  presents a pure dissociative potential which would allow for a direct map of the pumped NWP, as those performed in a number of previous works that use pump-probe schemes tracing molecular ions by its direct reflection into Coulomb repulsion curves [14, 15]. Such potentials allow one to take a direct snapshot of the NWP localization by inspecting the PKE spectrum of the ejected charged particles. A one-to-one correspondence of the measured PKE into  $R$  through the potential curve and by simply using the reflection approximation retrieves the NWP motion. This is shown in the right panels in Fig. 4, where we compare the calculated NWP at different time delays (green line with circles) and the NWP extracted from the  $2p\sigma_u$  contribution to the PKE (blue line with squares). Such a direct mapping can only be achieved theoretically in the present case, since separating in an experiment the contribution from each ionic state is not feasible and, as demonstrated in the PKE distributions, the  $2p\sigma_u$  state is a minor contribution, making it hard to extract.

However, one can take advantage of the fact that the two ionic states contributing to dissociative ionization have different parity. The coherent superposition of states of different parity lead to symmetry breaking in the electron ejection. Thus, despite the smaller amplitudes associated to one of the states involved, their coherent superposition can magnify its contribution. The electron angular distributions for eight different PKE and time delays are plotted in Fig 5(above). Each panel corresponds to a given PKE and contains the angular distributions computed for four different time delays (4, 6, 8 and 10 fs). As we scan the angular distributions for different KER, we find pronounced asymmetries for the time delays at which the absorption of the probe leads to a non-negligible contribution from the  $2p\sigma_u$ . Experimental measurements of the complete electron angular distributions are feasible [4], although difficult to obtain. Nevertheless, since the relevant information is the degree of asymmetry, one can define the asymmetry parameter as:

$$A = \frac{N_{up} - N_{down}}{N_{up} + N_{down}} \quad (8)$$

and consequently only measure the probability of ejecting an electron upwards (downwards) respect to the proton ejection [28], i.e integrating the electron angular distributions over the solid angle in the two semispheres defined by a plane perpendicular to the molecular axis that contains the inversion symmetry center. The resulting asymmetry parameter is plotted in Fig. 5(below) as a function of PKE (y-axis) and time-delay (x-axis). This produces a well defined pattern that traces the localization of the pumped NWP in time. For comparison, the ionization probability is plotted on the Fig. 5(above). We can see that the sudden sign change in the asymmetry parameter where the NWP is localized allows for a visible signature hardly measurable in the ionization probabilities.

#### 5. Conclusions

We investigate the use of a UV pump - UV probe scheme with two identical pulses to time-resolve the dynamics of a NWP in excited electronic states of  $\text{H}_2$ . The photon energies involved

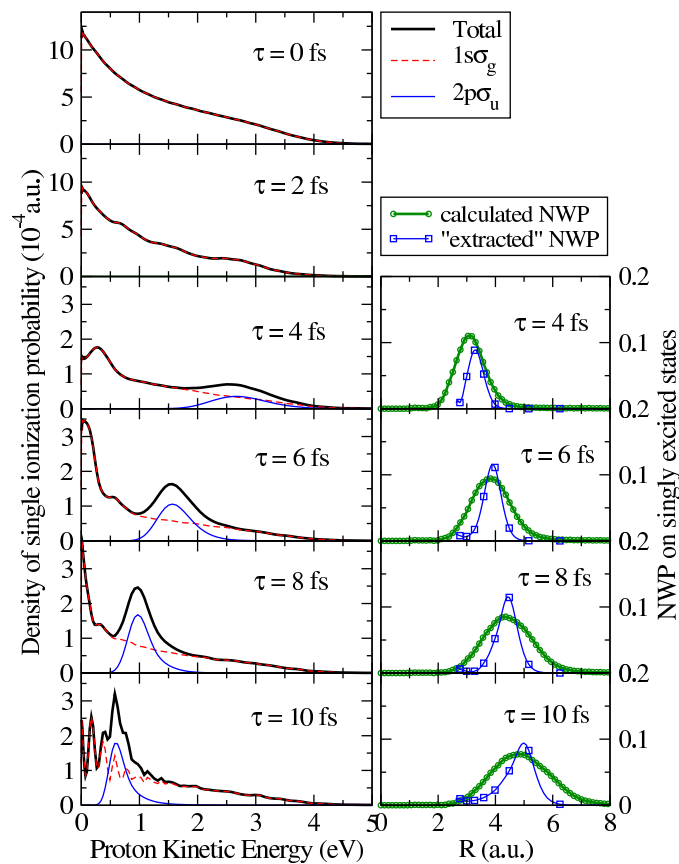


**Figure 4.** (Left column) Dissociative ionization probabilities as a function of the proton kinetic energy (PKE) release for different time delays. We also include the contributions from each ionization threshold: dashed red line corresponds to  $1s\sigma_g$  and full blue line corresponds to  $2p\sigma_u$  state of the molecular ion. (Right column) NWP obtained from the ab initio calculations at different times (thick green full line) compared with the reconstruction of the wave packet from the  $2p\sigma_u$  distribution as explained in the text.

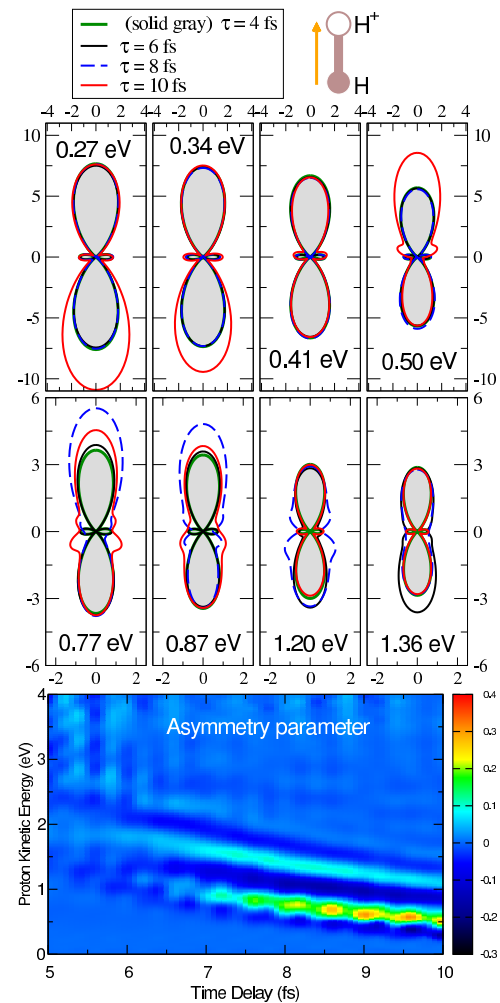


**Figure 5.** (Above) Electron angular distributions integrated over all electron energies at different time delays. Each panel corresponds to a given PKE. The probabilities are normalized to those of a time delay of 4 fs and values are given in units of  $10^{-5}$ . (Below) Asymmetry parameter as defined in Eq. (8) as a function of the proton kinetic energy (y-axis) and time delay (x-axis).

singly ionize the molecule through different ionization thresholds, which prevents one to obtain a direct mapping into the single ionization signal as those found for the Coulomb explosion in previous works with simple systems [14, 15]. Nevertheless, because the states of the molecular ion have different parity, their coherent superposition results in an asymmetry in the electron angular distributions magnifying the measurable signal and therefore allowing for a clean trace of the field-free evolution of the pumped wave packet.



## 6. References

- [1] Drescher M, Hentschel M, Kienberger R, Tempea G, Spielmann C, Reider G A, Corkum P B and Krausz F 2001 *Science* **291** 1923–1927
- [2] Hentschel M, Kienberger R, Spielmann C, Reider G A, Milosevic N, Brabec T, Corkum P, Heinzmann U, Drescher M and Krausz F 2001 *Nature* **414** 509–513
- [3] Sansone G, Benedetti E, Calegari F, Vozzi C, Avaldi L, Flammini R, Poletto L, Villoresi P, Altucci C, Velotta R, Stagira S, De Silvestri S and Nisoli M 2006 *Science* **314** 443–446
- [4] Ullrich J, Moshhammer R, Dorn A, D Rner R, Schmidt L P H and Schmidt-B Cking H 2003 *Reports on Progress in Physics* **66** 1463–1545
- [5] Bostedt C, Chapman H N, Costello J T, Crespo López-Urrutia J R, Düsterer S, Epp S W, Feldhaus J, Föhlisch A, Meyer M and Möller T 2009 *Nuclear Instruments and Methods in Physics Research Section A: Accelerators, Spectrometers, Detectors and Associated Equipment* **601** 108–122
- [6] Barty A 2010 *Journal of Physics B: Atomic, Molecular and Optical Physics* **43** 194014
- [7] Krausz F and Ivanov M 2009 *Rev. Mod. Phys.* **81** 163–234
- [8] Goulielmakis E, Loh Z H, Wirth A, Santra R, Rohringer N, Yakovlev V S, Zherebtsov S, Pfeifer T, Azzeer A M, Kling M F, Leone S R and Krausz F 2010 *Nature* **466** 739–43
- [9] Calvert C, Bryan W, Newell W and Williams I 2010 *Physics Reports* **491** 1 – 28
- [10] Posthumus J H 2004 *Reports on Progress in Physics* **67** 623
- [11] Sansone G, Kelkensberg F, Pérez-Torres J F, Morales F, Kling M F, Siu W, Ghafur O, Johnsson P, Swoboda M, Benedetti E, Ferrari F, Lépine F, Sanz-Vicario J L, Zherebtsov S, Znakovskaya I, L’Huillier a, Ivanov M Y, Nisoli M, Martín F and Vrakking M J J 2010 *Nature* **465** 763–766
- [12] Singh K P, He F, Ranitovic P, Cao W, De S, Ray D, Chen S, Thumm U, Becker A, Murnane M M, Kapteyn H C, Litvinyuk I V and Cocke C L 2010 *Physical Review Letters* **104** 1–4
- [13] Kelkensberg F, Siu W, Pérez-Torres J F, Morales F, Gademann G, Rouzée A, Johnsson P, Lucchini M, Calegari F, Sanz-Vicario J L, Martín F and Vrakking M J J 2011 *Phys. Rev. Lett.* **107**(4) 043002
- [14] Jiang Y H, Rudenko a, Pérez-Torres J F, Herrwerth O, Foucar L, Kurka M, Kühnel K U, Toppin M, Plésiat E, Morales F, Martín F, Lezius M, Kling M F, Jahnke T, Dörner R, Sanz-Vicario J L, van Tilborg J, Belkacem a, Schulz M, Ueda K, Zouros T J M, Düsterer S, Treusch R, Schröter C D, Moshhammer R and Ullrich J 2010 *Physical Review A* **81** 1–4
- [15] Jiang Y H, Rudenko a, Plésiat E, Foucar L, Kurka M, Kühnel K U, Ergler T, Pérez-Torres J F, Martín F, Herrwerth O, Lezius M, Kling M F, Titze J, Jahnke T, Dörner R, Sanz-Vicario J L, Schöffler M, van Tilborg J, Belkacem a, Ueda K, Zouros T J M, Düsterer S, Treusch R, Schröter C D, Moshhammer R and Ullrich J 2010 *Physical Review A* **81** 1–4
- [16] González-Castrillo A, Palacios A, Bachau H and Martín F 2012 *Phys. Rev. Lett.* **108** 063009
- [17] Tzallas P, Skantzakis E, Nikolopoulos L a a, Tsakiris G D and Charalambidis D 2011 *Nature Physics* **7** 781–784
- [18] Palacios A, Bachau H and Martin F 2006 *Physical Review A* **74** 1–4
- [19] Sanz-Vicario J, Bachau H and Martín F 2006 *Physical Review A* **73** 1–12
- [20] Sánchez I and Martín F 1997 *The Journal of Chemical Physics* **106** 7720
- [21] Martín F 1999 *Journal of Physics B: Atomic, Molecular and Optical Physics* **32** R197
- [22] Balay S, Brown J, Buschelman K, Gropp W D, Kaushik D, Knepley M G, McInnes L C, Smith B F and Zhang H 2011 PETSc Web page <http://www.mcs.anl.gov/petsc>
- [23] Feshbach H 1962 *Ann. Phys.* **19** 287–313
- [24] Cortés M and Martín F 1994 *Journal of Physics B: Atomic, Molecular and Optical Physics* **27** 5741
- [25] Bachau H, Cormier E, Decleva P, Hansen J E and Martín F 2001 *Reports on Progress in Physics* **64** 1815
- [26] Palacios A, Bachau H and Martín F 2005 *Journal of Physics B: Atomic, Molecular and Optical Physics* **38** L99
- [27] Wolniewicz L and Staszewska G 2003 *J. Mol. Spectrosc.* **217** 181–185
- [28] Fischer A, Sperl A, Cörlin P, Schönwald M, Rietz H, Palacios A, González-Castrillo A, Martín F, Pfeifer T, Ullrich J, Senftleben A and Moshhammer R 2013 *Phys. Rev. Lett.* **110**(21) 213002